Core Phases Observed with AlpArray

On Ki Angel Ling[1], Simon Stähler[1], Domenico Giardini[1], Kasra Hosseini[2], and the AlpArray Working Group[3]

[1] Institute of Geophysics, ETH Zürich, Zurich, Switzerland (angel.ling@erdw.ethz.ch)

[2] The Alan Turing Institute, London, UK

[3] www.alparray.ethz.ch

Motivations: Challenges in Mantle Tomography

Most seismic tomographic models have a lower resolution in the mantle below 1000 km due to the following challenges in mantle tomography:

- The distribution of earthquakes and the ray paths of their main body waves is non-uniform.
- The sampling in the lowermost mantle is limited because of the narrow incidence angle range of the main body waves.

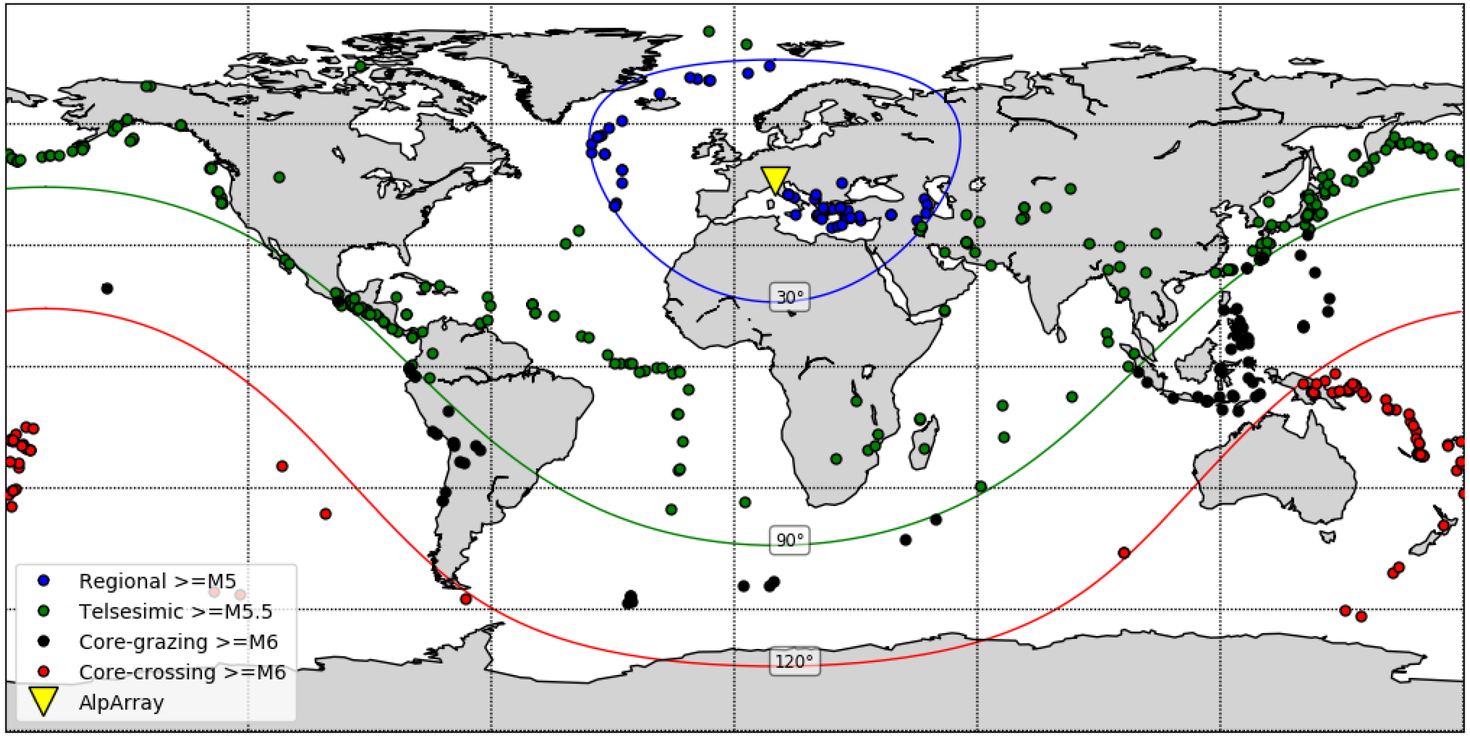

Figure 1: Global earthquake map between 2017-2018.
Blue: regional EQs (≥M5) within 30° epicentral distance of AlpArray;
Green: teleseismic EQs (≥M5.5) between 30-90° distance;
Black: EQs (≥M6) in core-grazing distance (90-120°);
Red: EQs (≥M6) in core-crossing distance (>120°).

Motivations: Core Phases

Previous studies (e.g. *Zhao 2019, Hosseini, et al., 2019*) have demonstrated the importance of **core-interacting seismic phases** in seismic tomography by:

- Increasing ray path coverage
- Constraining mid- and lower mantle structures

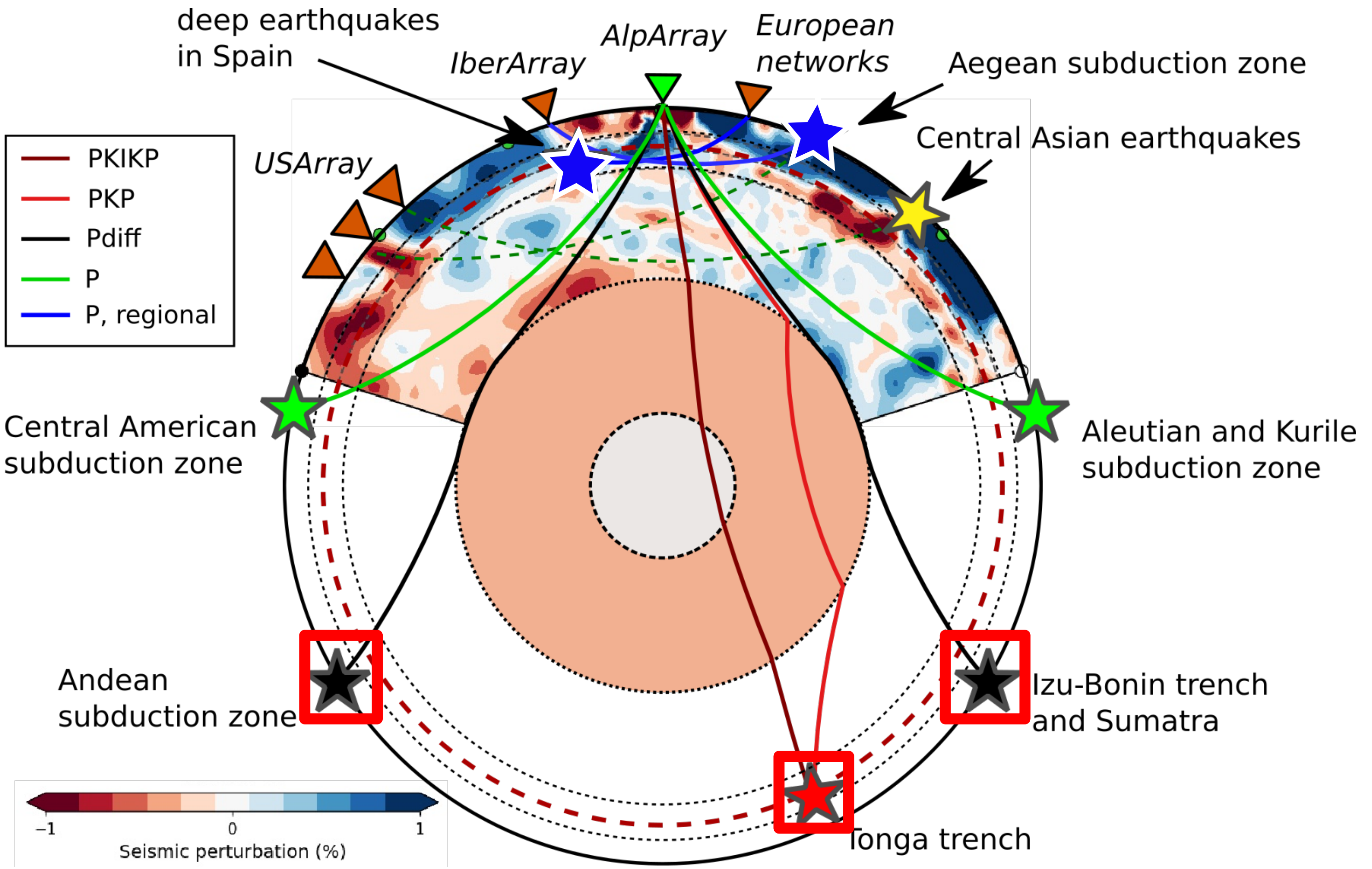

Figure 2: Ray paths of the some seismic phases that can be observed by AlpArray. Background model is the global multi-frequency P-wave model from *Hosseini, 2016*.

Motivations: AlpArray Initiative

The AlpArray Seismic Network (AASN)

- 2016-2019
- ~630 stations (including 30 OBS)
- Station spacing <52 km
- Provide high-resolution, large-aperture seismological data
- Observe seismic phases coming from all directions

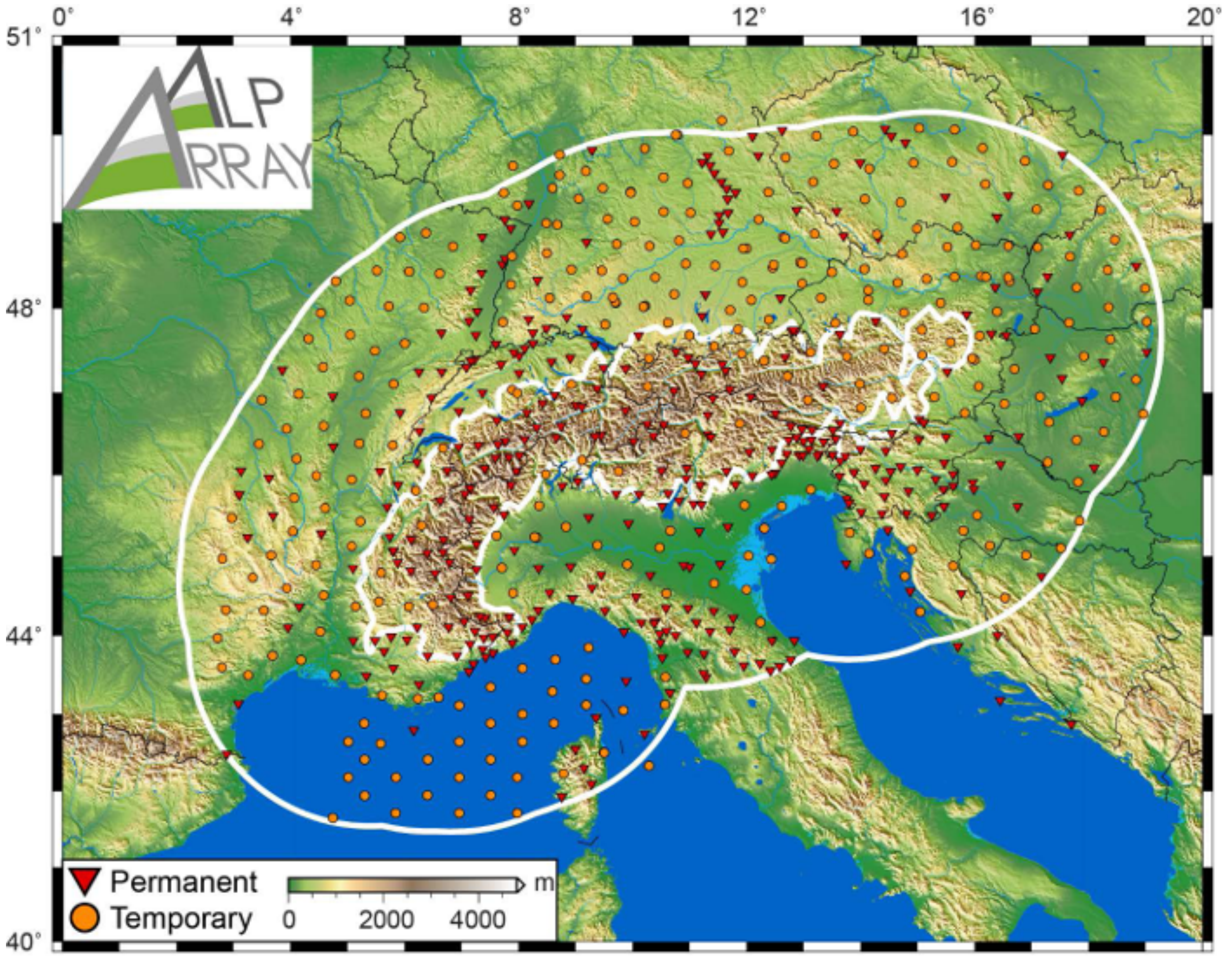

Figure 3: Station map of AlpArray Seismic Network (http://www.alparray.ethz.ch)

Goals

Investigate the visibility of core phases observed with AlpArray and determine their usability in future seismic waveform tomographic studies.

1. Apply array processing techniques to identify core phases with different slownesses.

2. Assess the availability of these core phases and analyze their characteristics in different frequency ranges.

Approach

- Download and pre-process AASN stations and stations in the neighboring local networks using ObspyDMT (*Hosseini and Sigloch, 2017*).
- Identify core phases observed from **core-crossing** (>120°) and **teleseismic** (30-90°) distances.
- Results are shown in phase aligned record sections and 4th-root vespagrams.

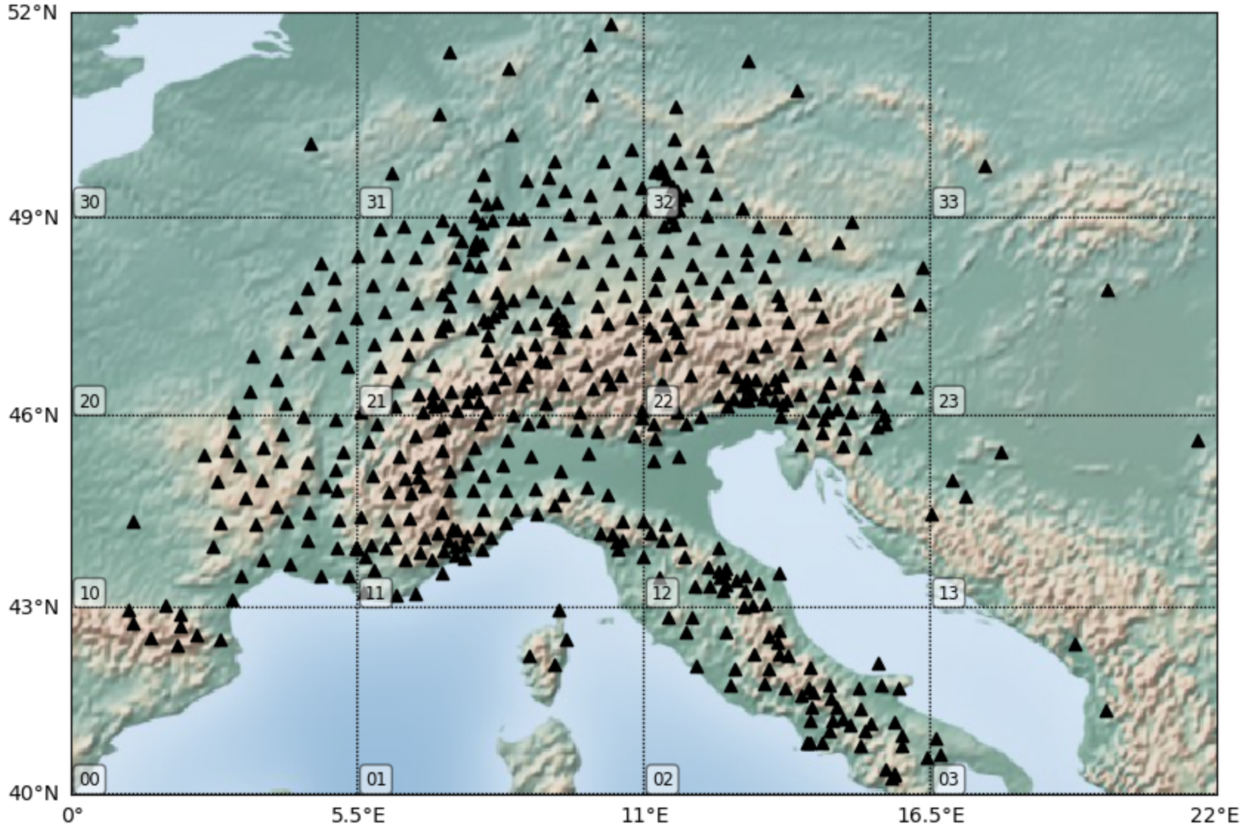

Figure 4: Map of stations that are used to identify core phases.

Results: Observed from Core-crossing Distances

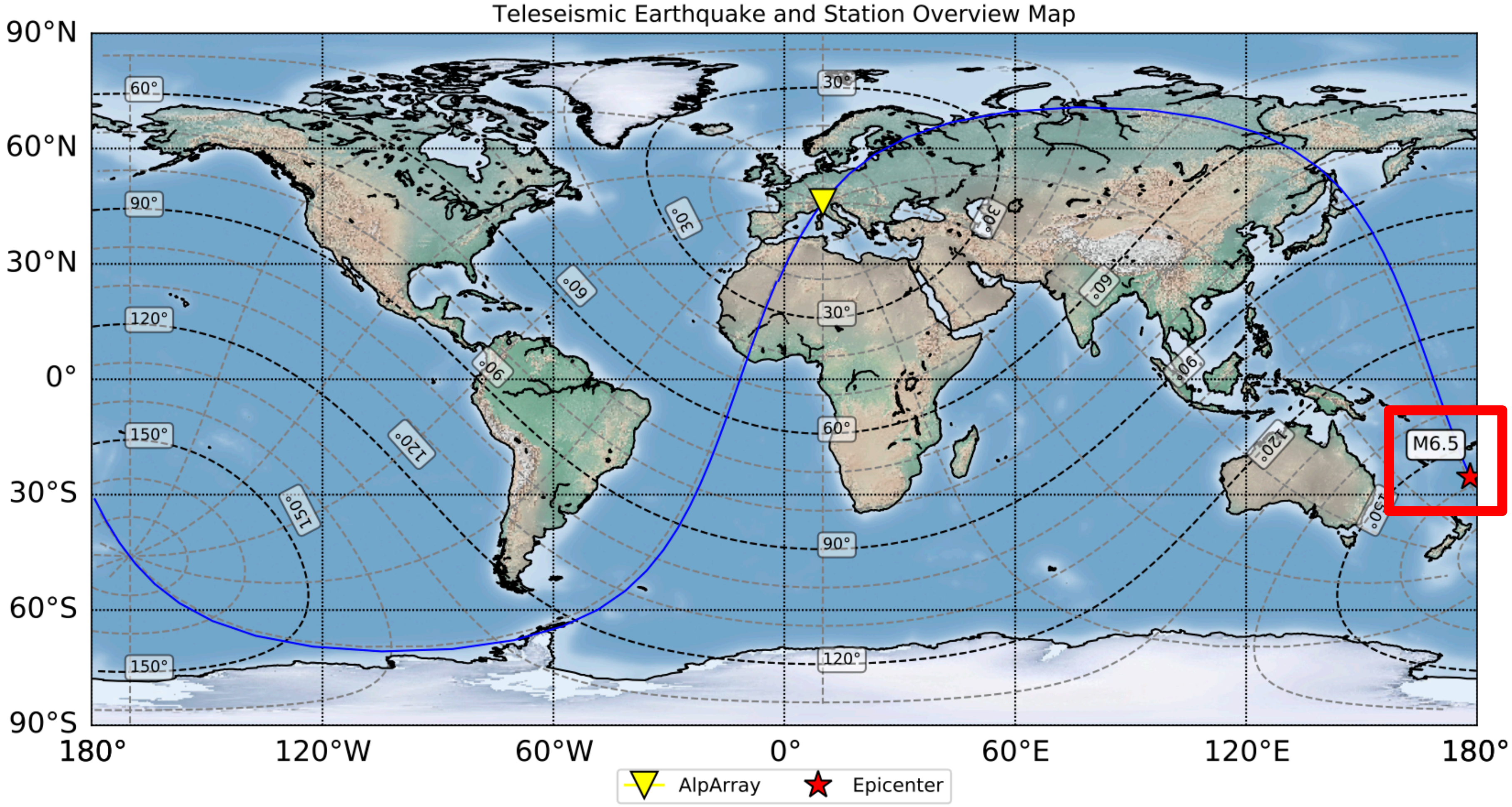

Figure 5: An overview map showing the location of AlpArray (**yellow** triangle), the selected example earthquake (M6.5, **red** star) in the Fiji region, and its backazimuth line (**blue**).

PKIKP and PKP

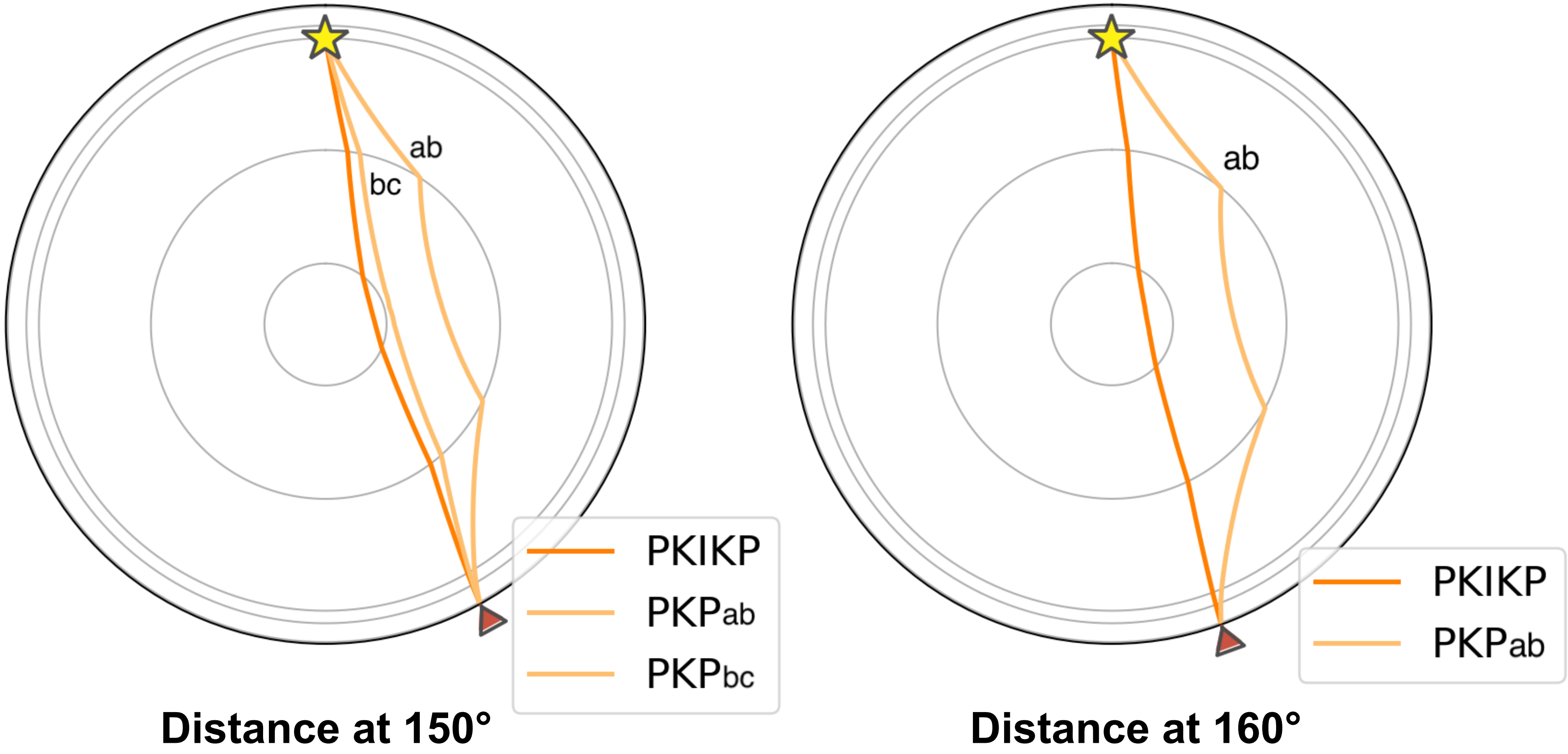

Figure 6: Ray paths of PKIKP (PKPdf) and PKP (PKPab and PKPbc).

- Core-refracted P
- Steep incidence angle
  - < 15°
- Well-observed from a core-crossing distance
- If we want to include these phases in tomography, we must ensure that they can be modelled accurately.

PKIKP and PKP: Fiji M6.5, Depth 576km

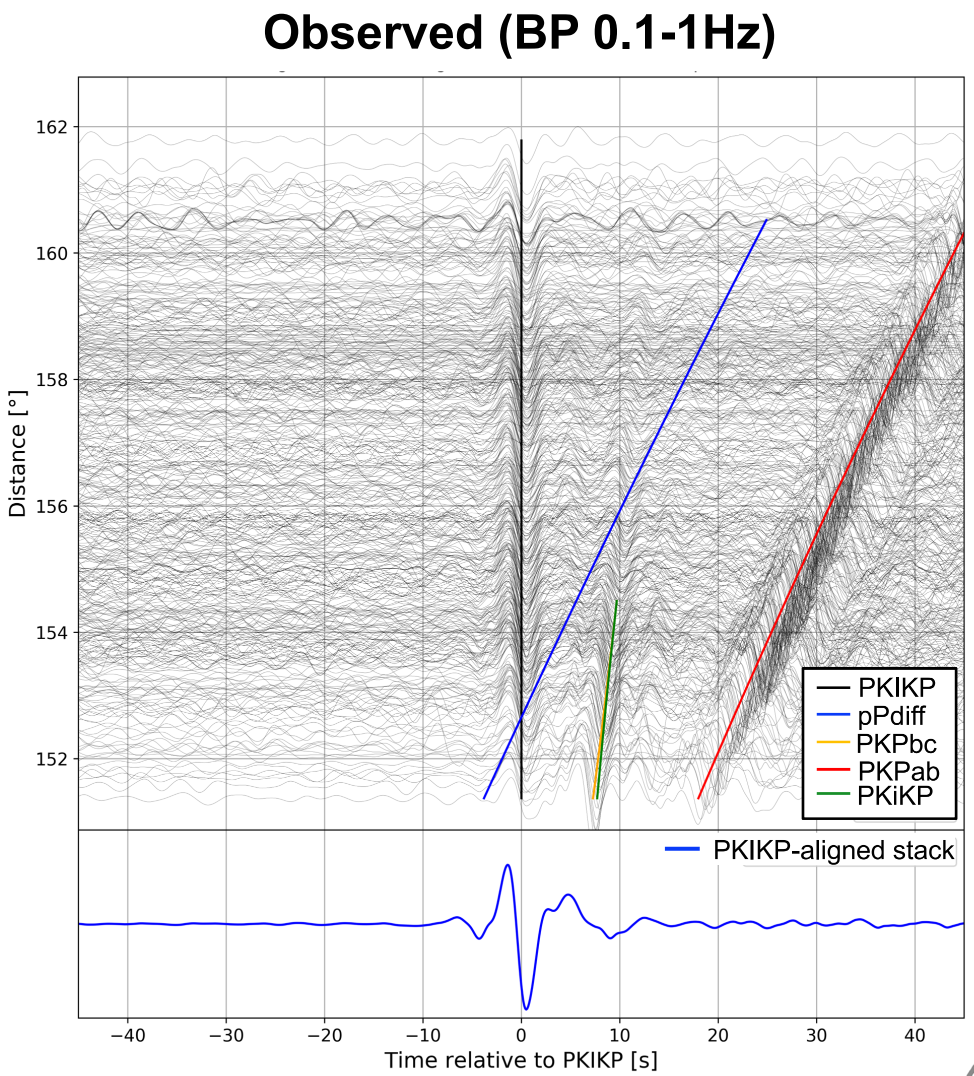

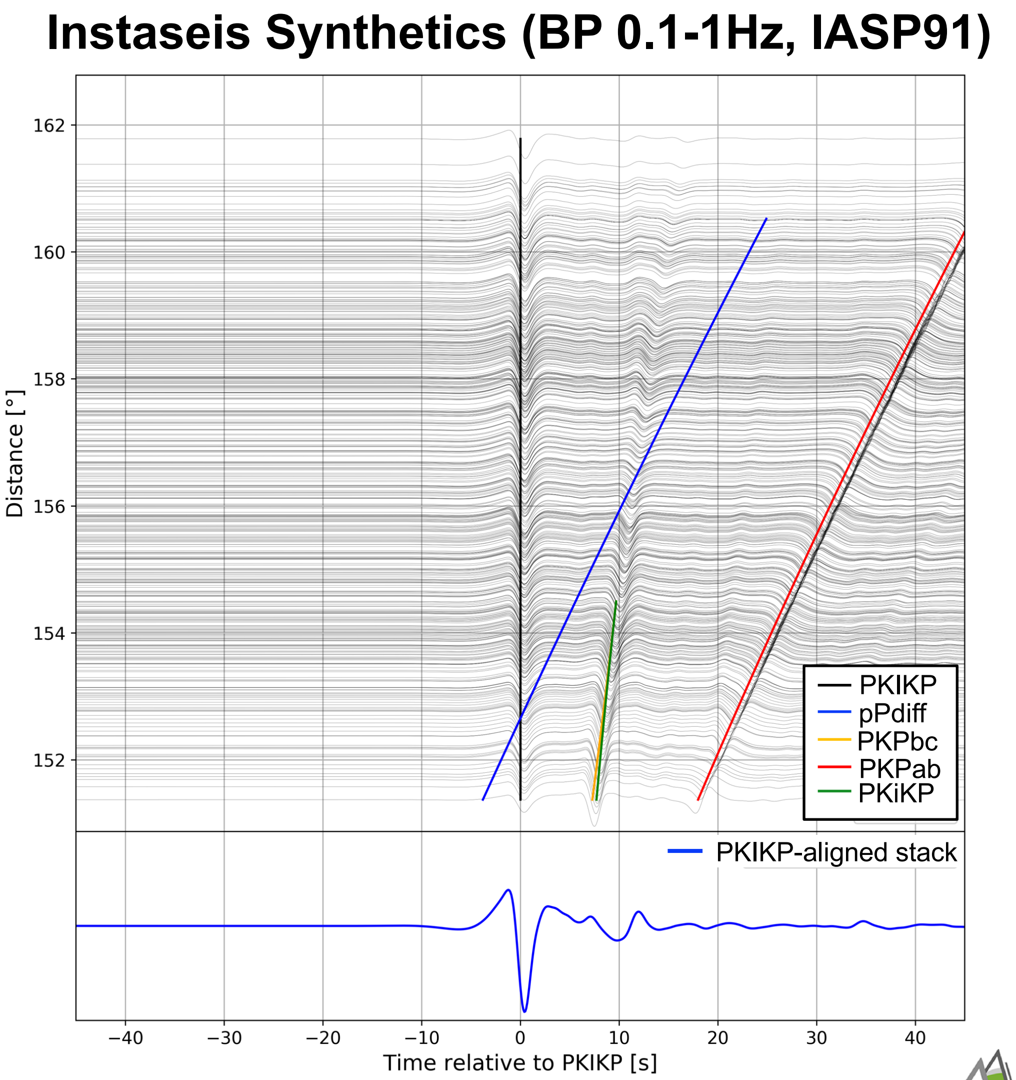

Figure 7: Vertical sections of the bandpassed observed (left) and synthetic waveforms (right) aligned to PKIKP.

PKIKP and PKP: Fiji M6.5, Depth 576km

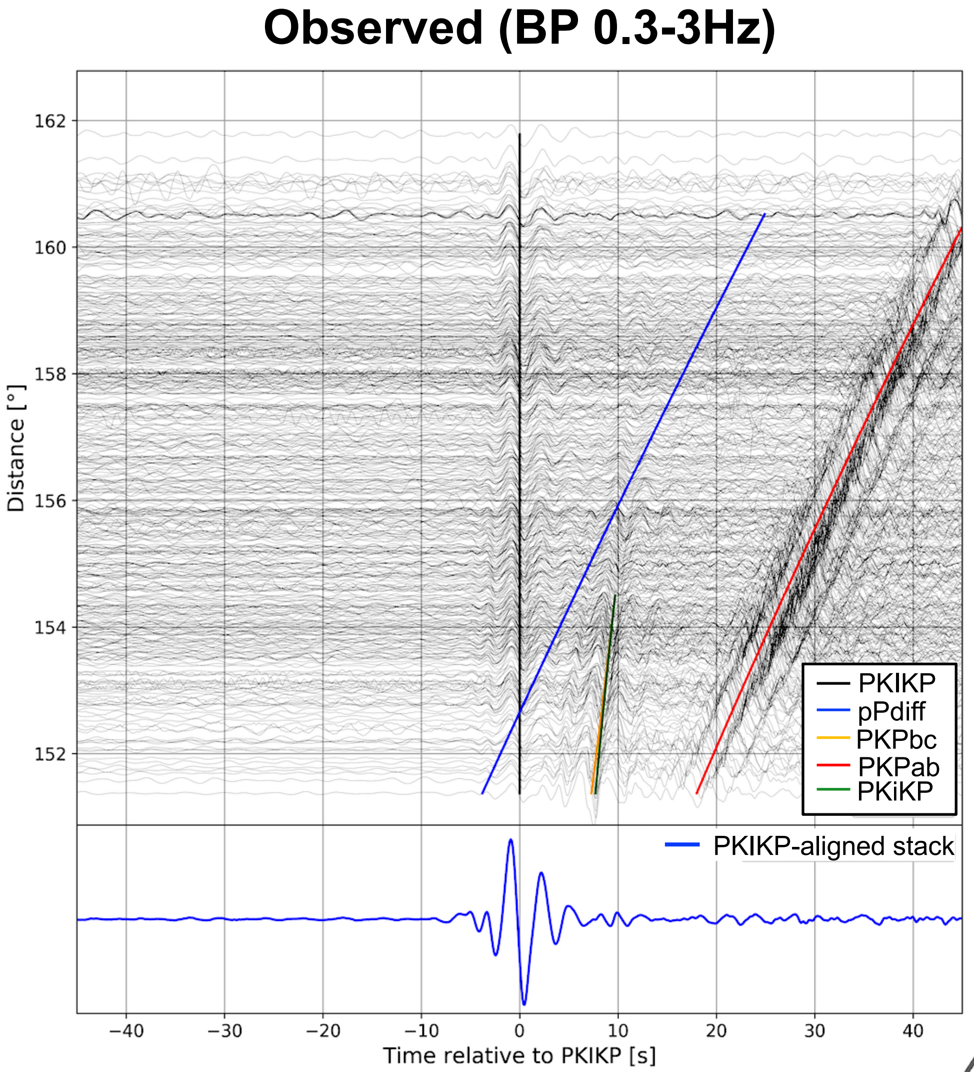

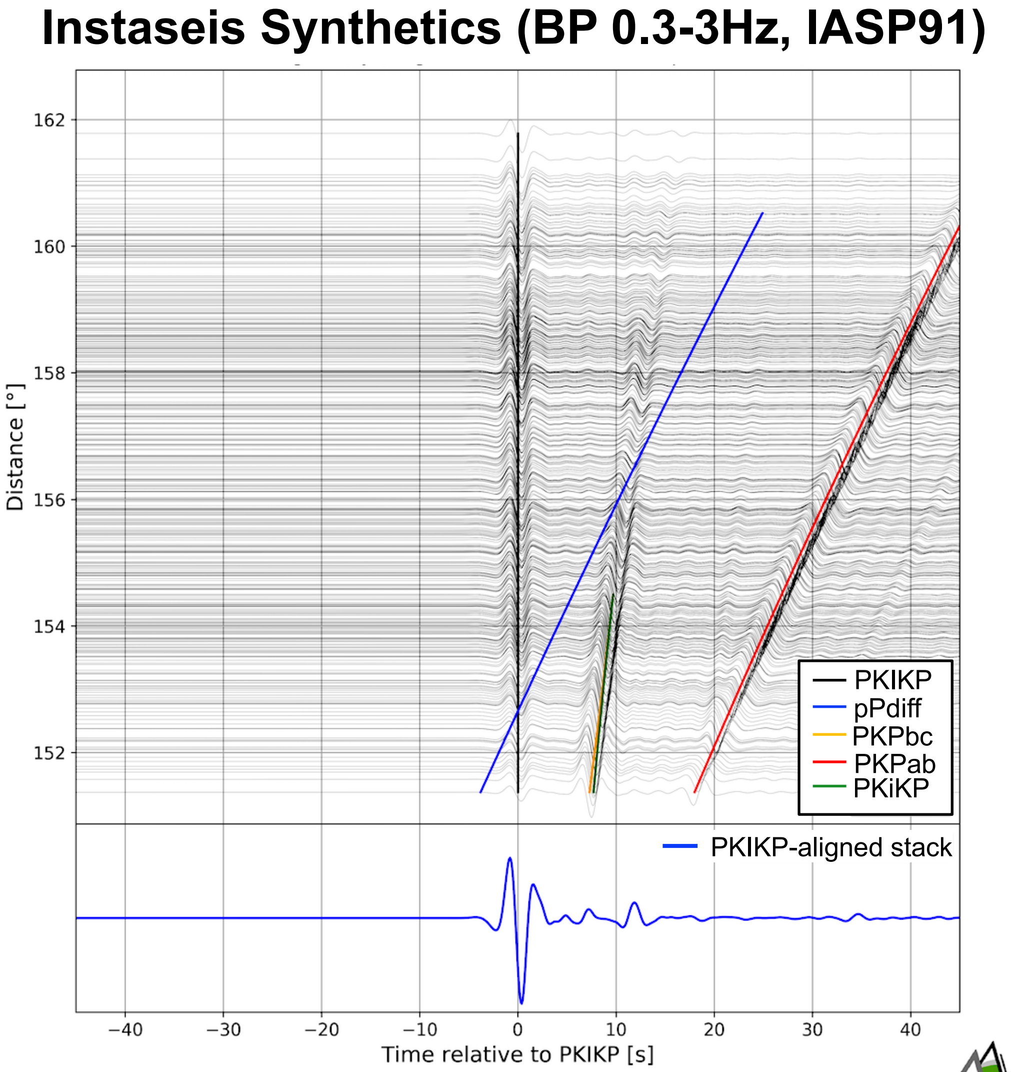

Figure 8: Vertical sections of the bandpassed observed (left) and synthetic waveforms (right) aligned to PKIKP.

Results: Observed from Teleseismic Distances

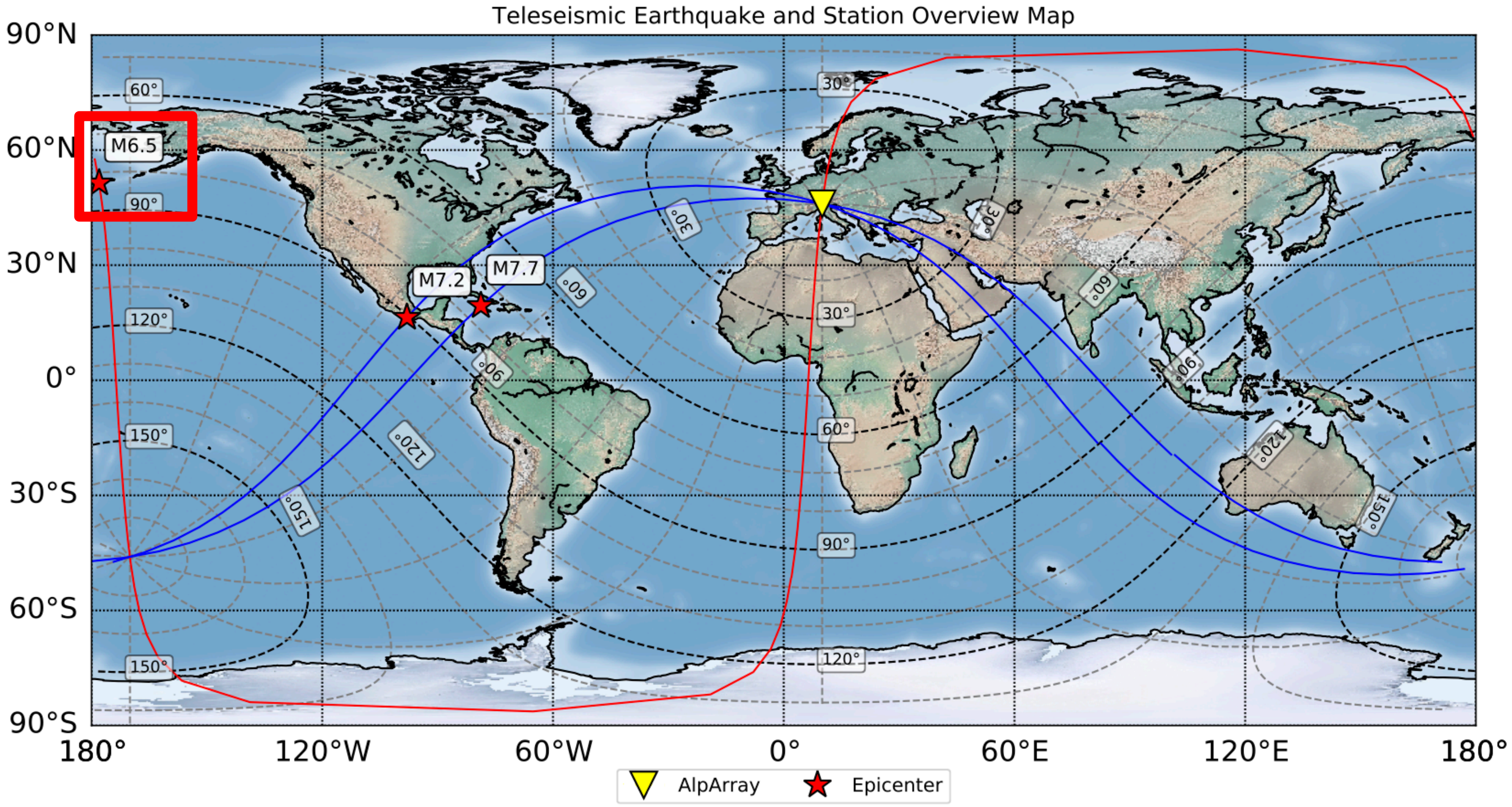

Figure 9: An overview map showing the location of AlpArray (**yellow** triangle), the 3 selected example earthquakes (**red** stars) in Alaska (M6.5), Mexico (M7.9) and Cuba (M7.2), and their backazimuth lines (**red**: ccK/SKP.K is observed; **blue**: ccK/ SKP.K is not observed)

High Order Core Phases

- The observed waveforms are filtered and aligned to the first P wave.
- The resulted record section exhibits some high order core phases that can be observed from teleseismic events.
- To verify the existence of these core phases, 4th-root vespagrams are computed to better constrain their slowness.

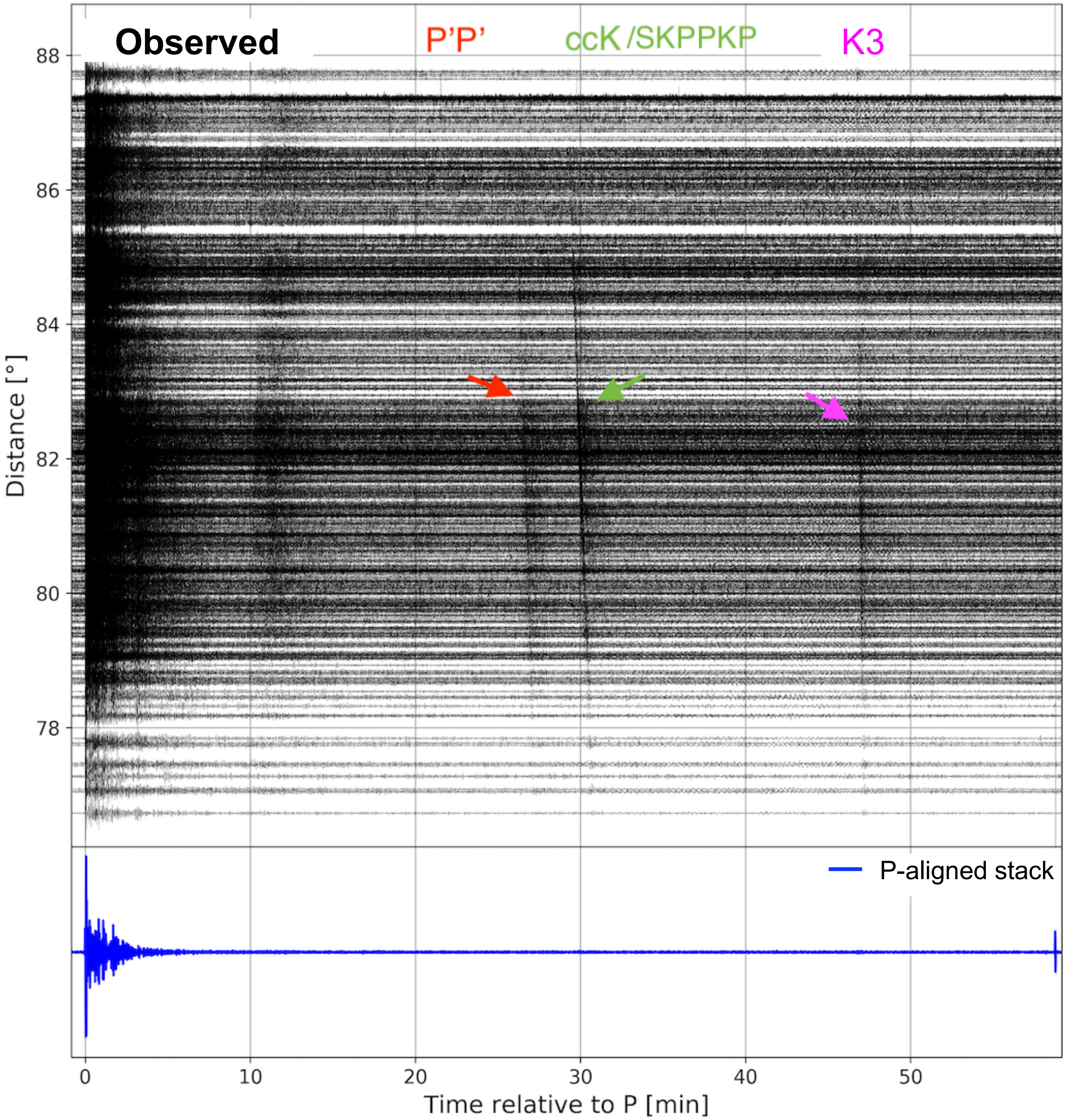

Figure 10: A 60-min vertical section of the observed waveforms (BP 0.3-3Hz) of the Alaskan event aligned to P.

PKIKPPKIKP (P'P'): Alaska M6.5, Depth 33.9km

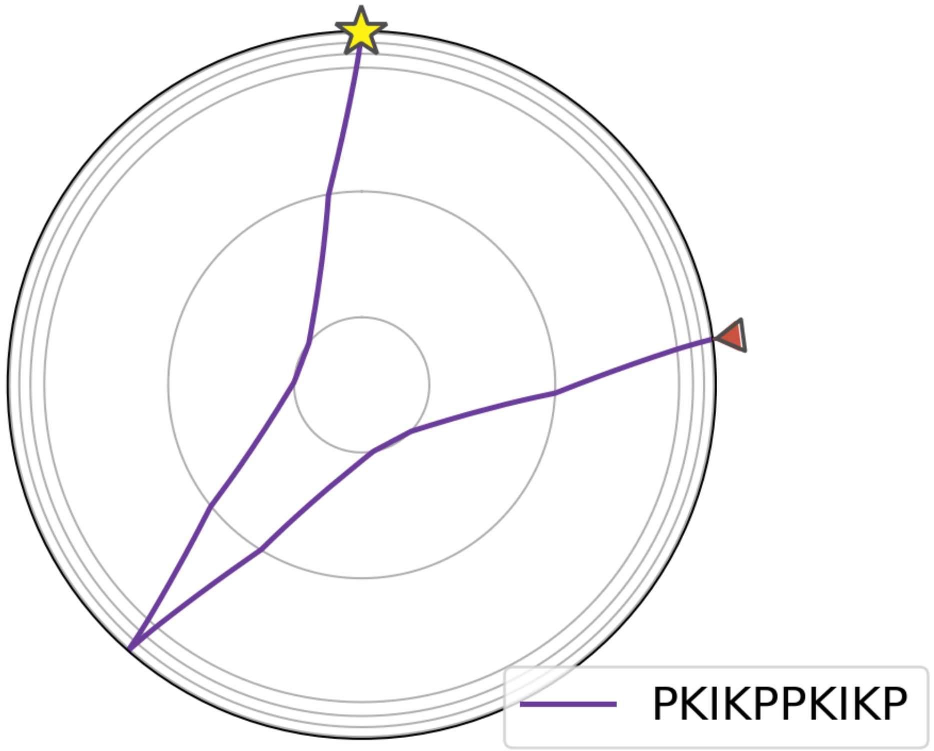

Distance at 82°

Figure 11: Ray path of PKIKPPKIKP. Similar to PKIKP, it has steep incidence angle.

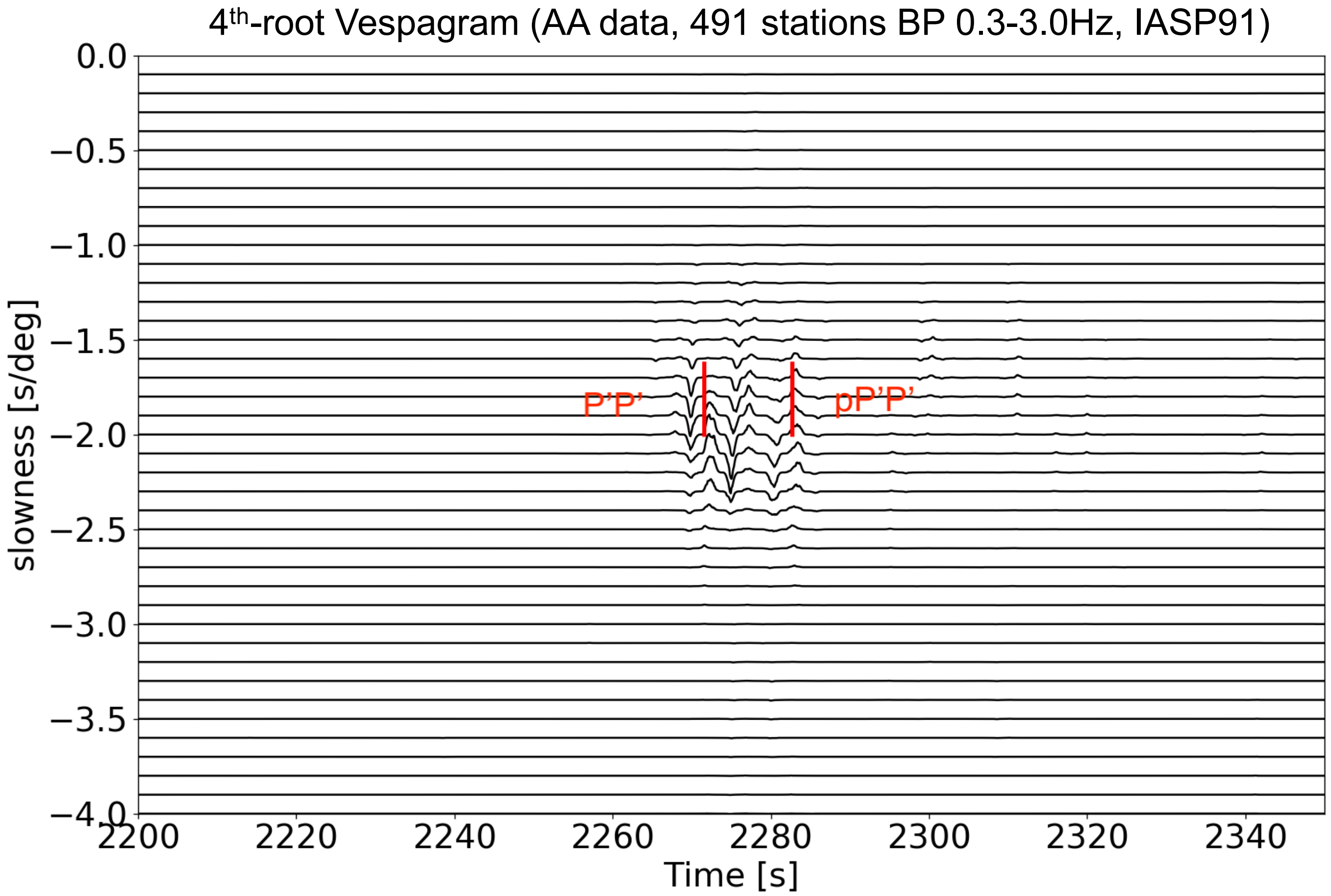

Figure 12: Vespagram of P'P' and the depth phase pP'P. The red vertical lines indicate their theoretical slowness based on the reference model IASP91 across the array. The small negative slowness indicates an opposite ray path to the main P wave and a steep incidence angle.

PKPPKPPKP (K3): Alaska M6.5, Depth 33.9km

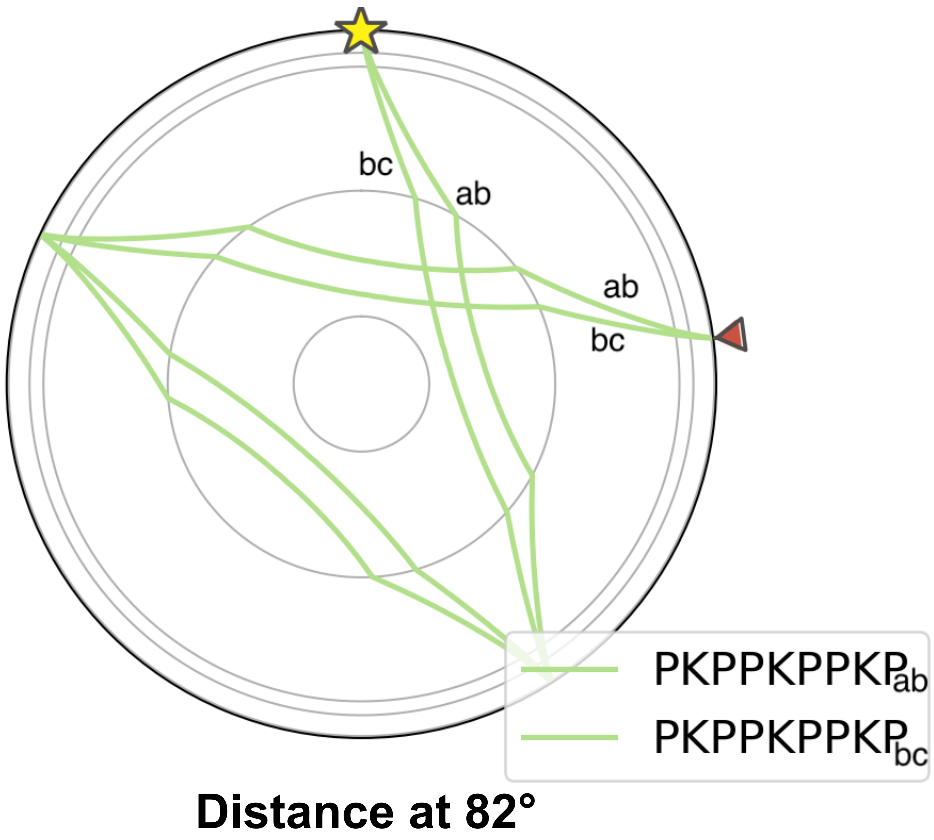

Figure 13: Ray path of PKPPKPPKP. Similar to PKP, this phase is split into two branches with different slownesses and steep incidence angle.

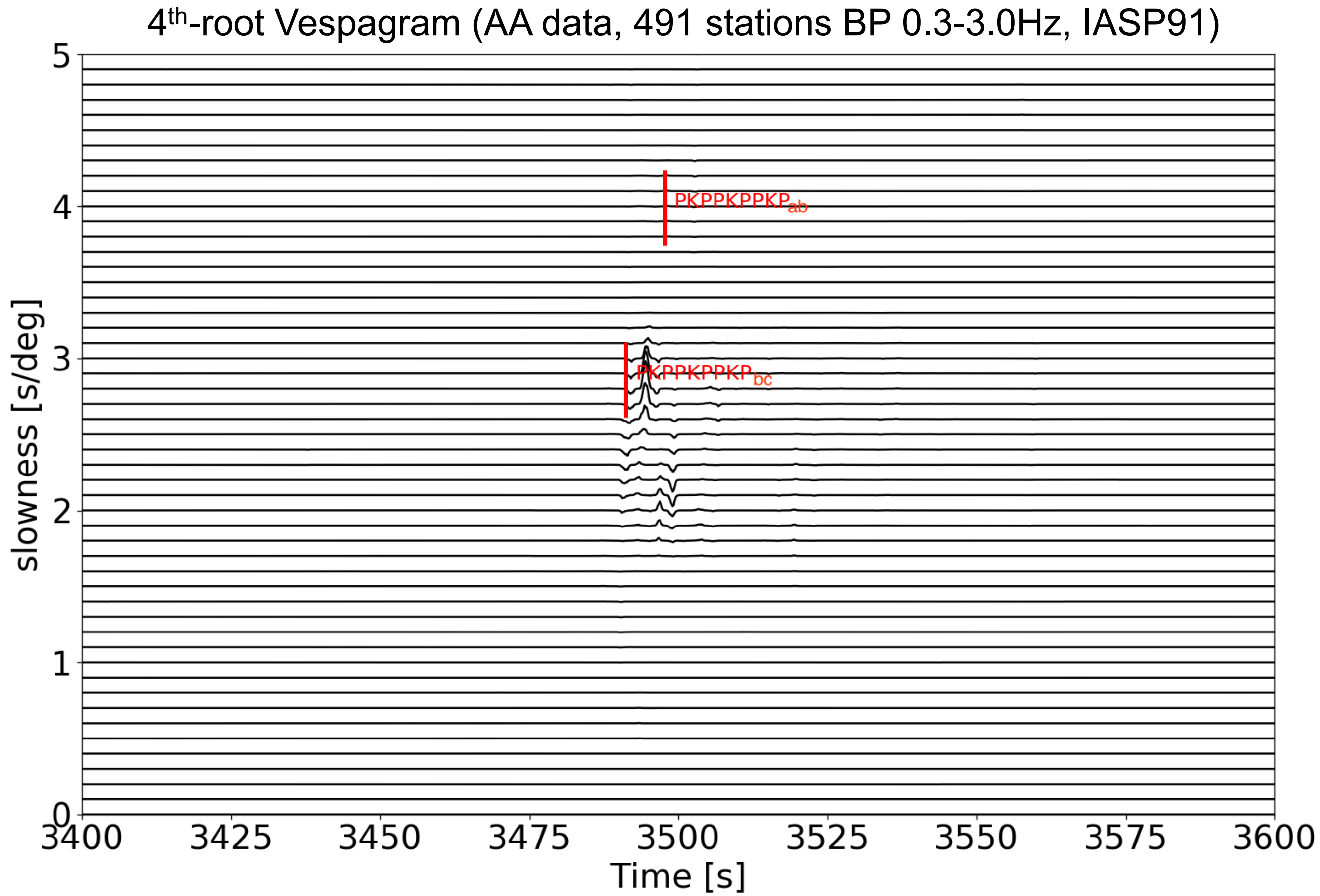

Figure 14: Vespagram of PKPPKPPKPab and PKPPKPPKPbc. The red vertical lines indicate their theoretical slowness based on the reference model IASP91 across the array. Only PKPPKPPKPbc is observed by AlpArray.

PcPPcPPKP (ccK) / SKPPKP (SKP.K)

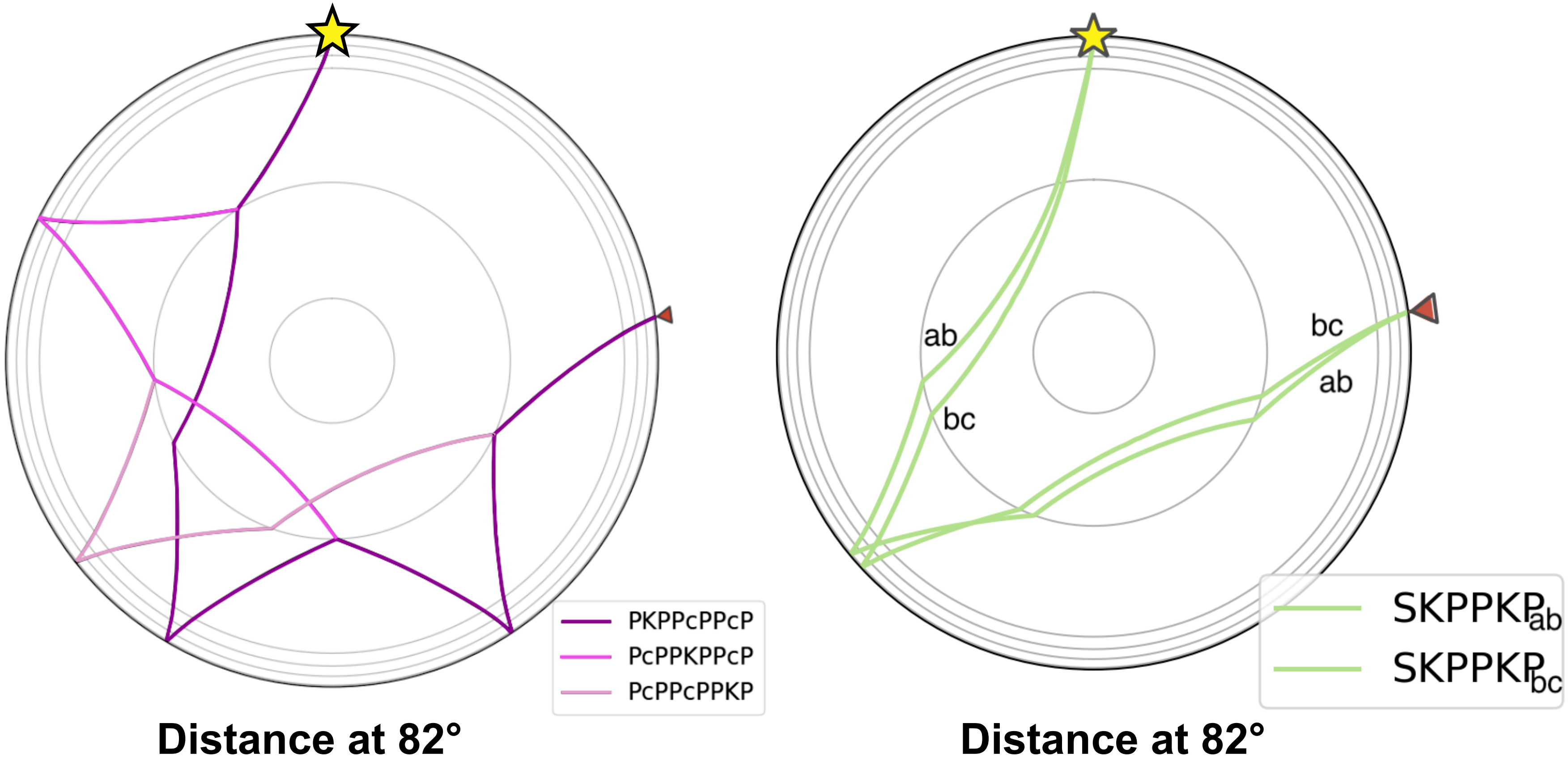

Figure 15: Ray paths of PcPPcPPKP and SKPPKP.

- Steep incidence angle
- Different ray path orders with the same theoretical arrival time
- Multiple interaction points at CMB with the same/similar locations
- Small differential traveltime btw. 55-85°

PcPPcPPKP (ccK) / SKPPKP (SKP.K)

Alaska M6.5, Depth 33.9km

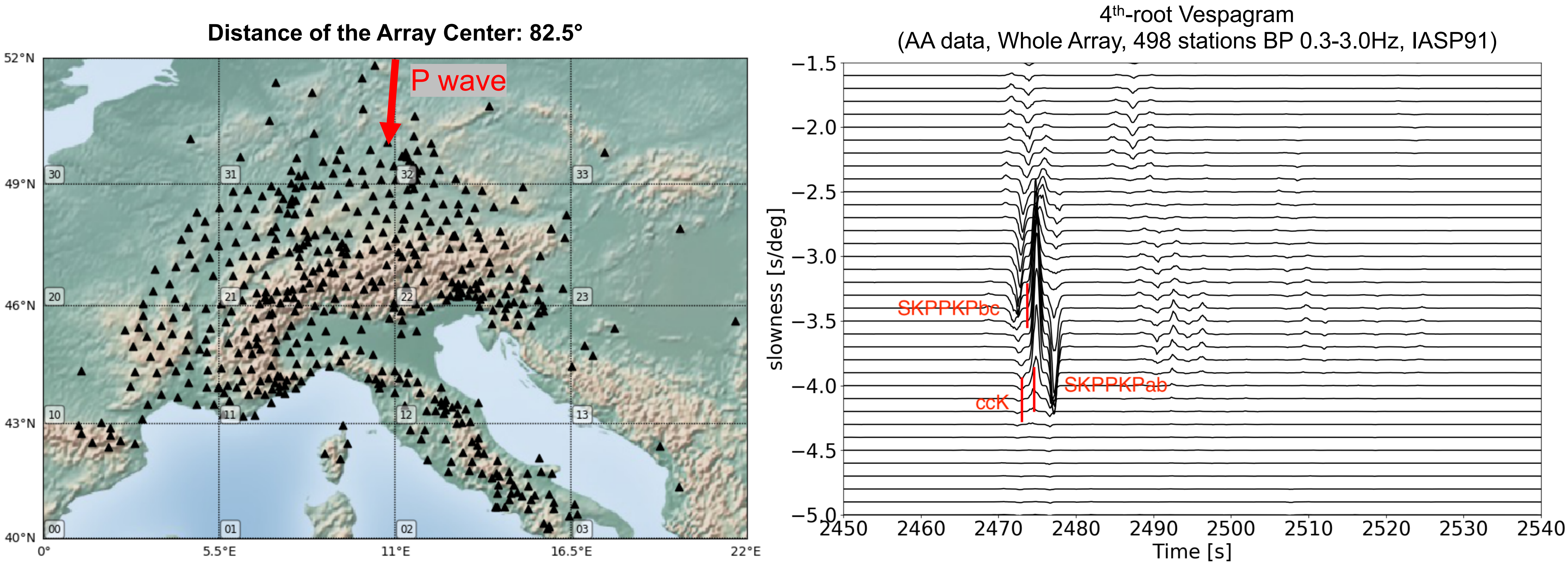

Figure 16: Vespagram of ccK and SKP.K computed using the whole array. The red vertical lines indicate their theoretical slowness based on the reference model IASP91 across the array. The red arrow here is showing the direction of the direct body waves arriving at the array. We can see all three phases and SKP.K BC branch has largest amplitude of all.

PcPPcPPKP (ccK) / SKPPKP (SKP.K)

Alaska M6.5, Depth 33.9km

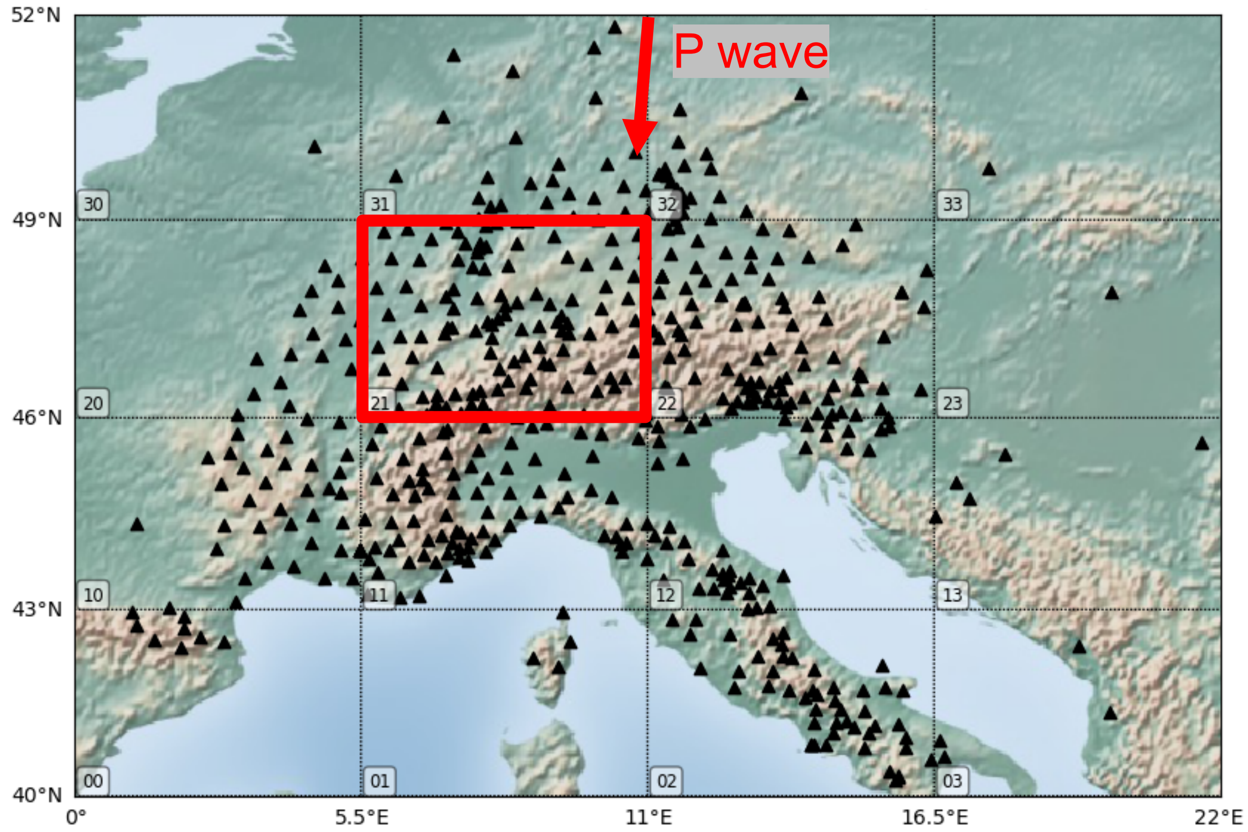

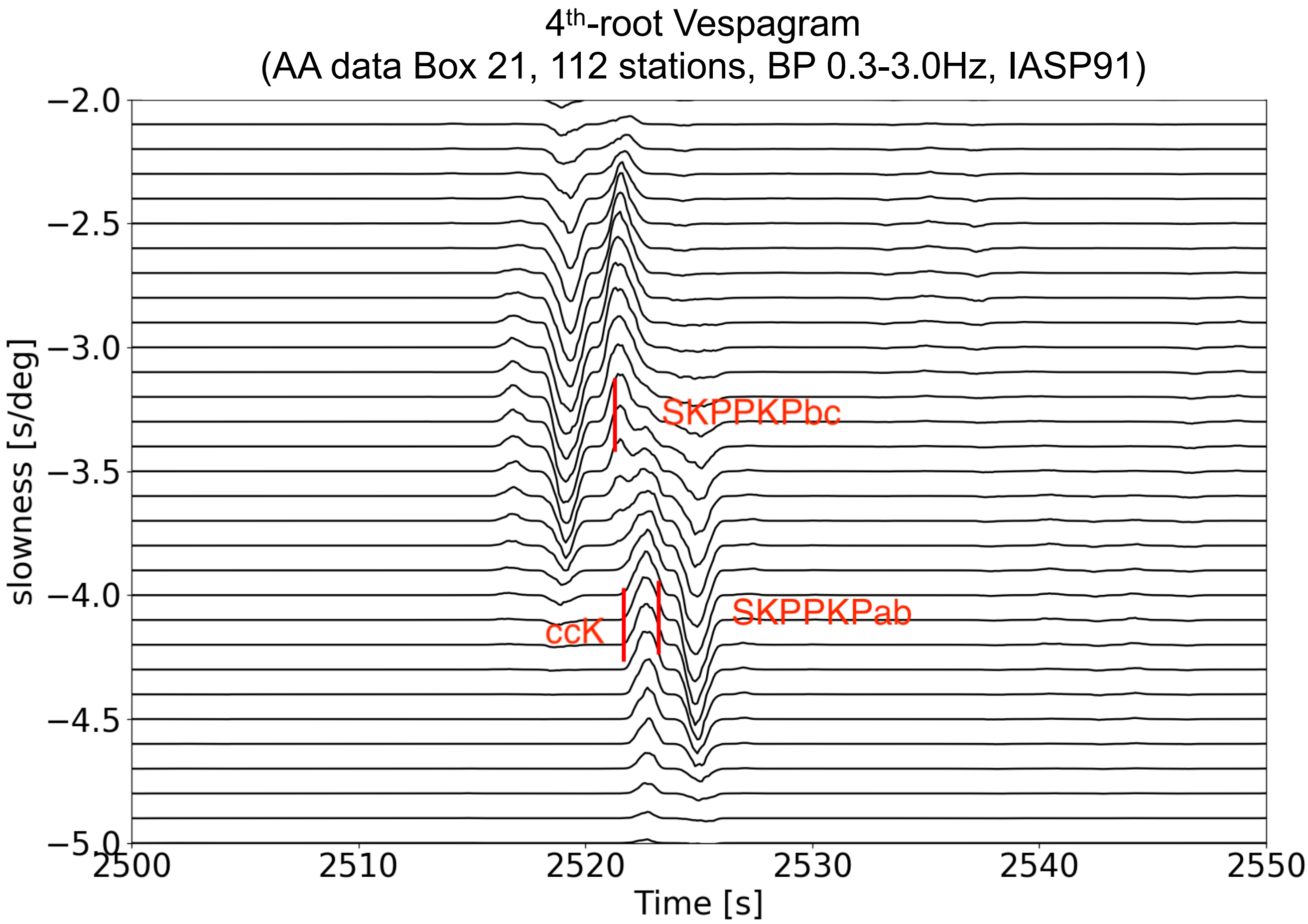

Figure 17: AlpArray can be divided into subarrays to investigate arrivals and behavior of core phases in different distance range. Here the subarray closer to the center of the whole array is chosen. The differential traveltime of SKP.Kbc and ccK are very close, but since they have different velocities, we can easily observe and identify them on vespagram.

PcPPcPPKP (ccK) / SKPPKP (SKP.K)

Alaska M6.5, Depth 33.9km

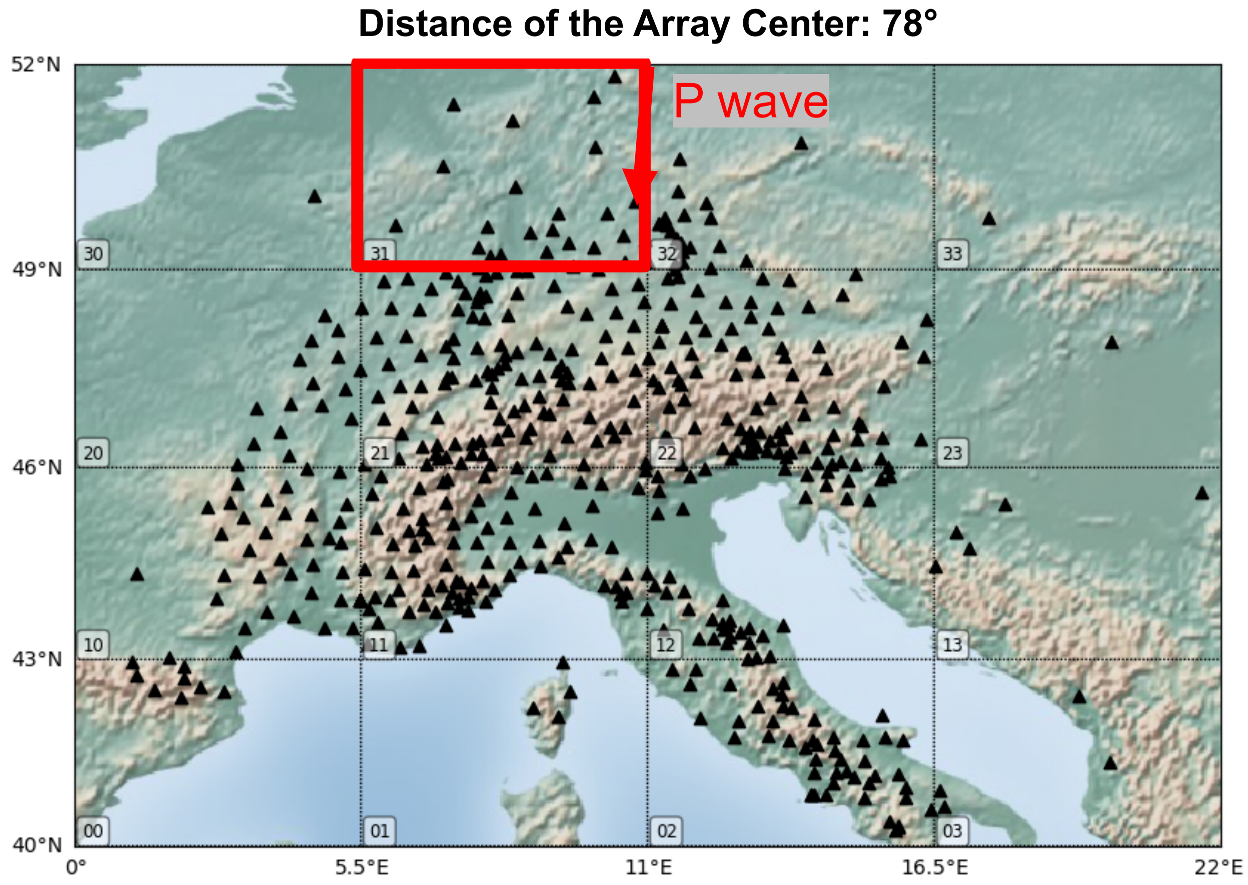

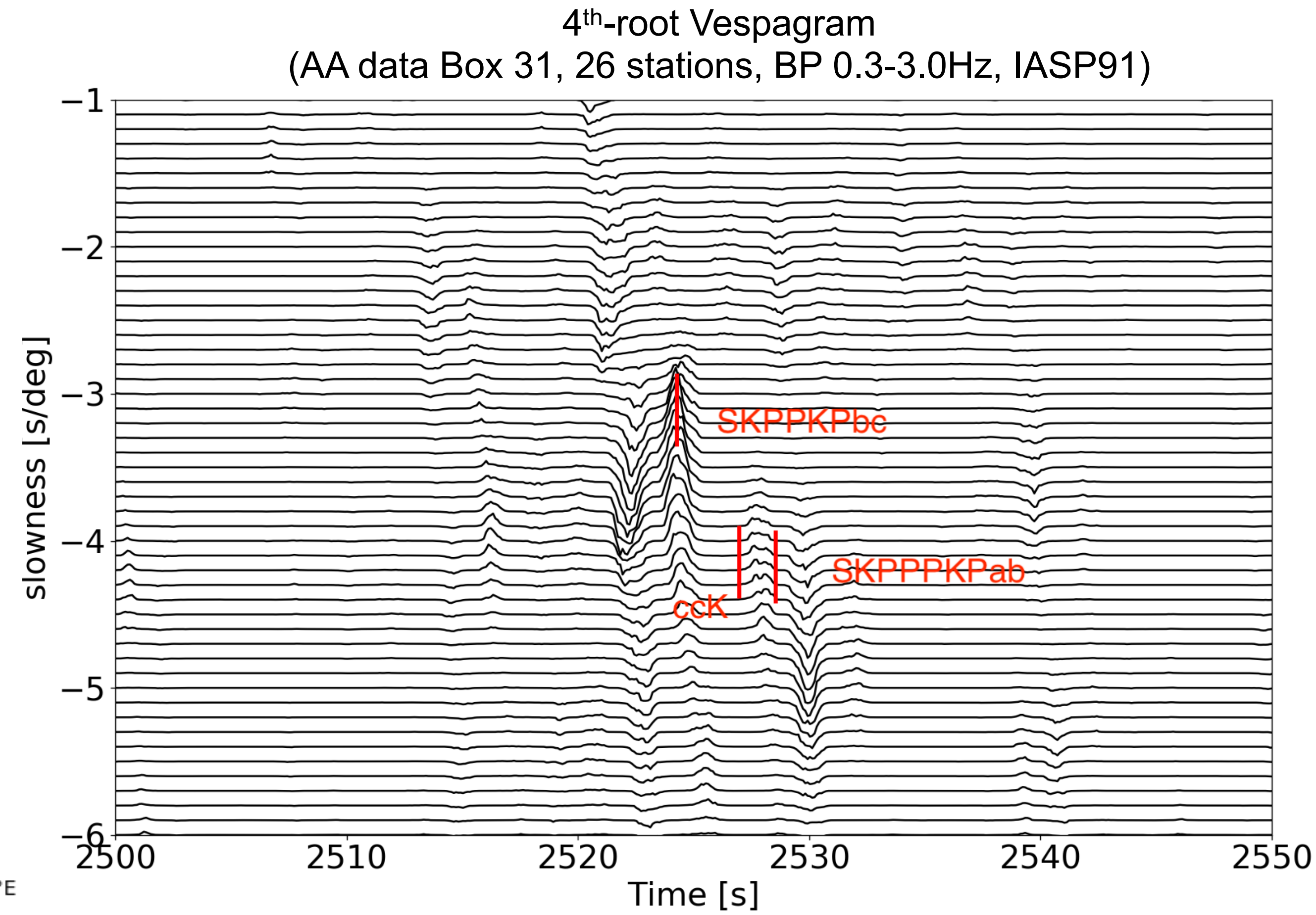

Figure 18: Here the subarray closer to the event is chosen. The differential traveltime of SKP.Kbc and ccK is now larger. In this distance range, ccK has a smaller amplitude compared to the one observed in the subarray closer to the center of the whole array.

PcPPcPPKP (ccK) / SKPPKP (SKP.K)

Alaska M6.5, Depth 33.9km

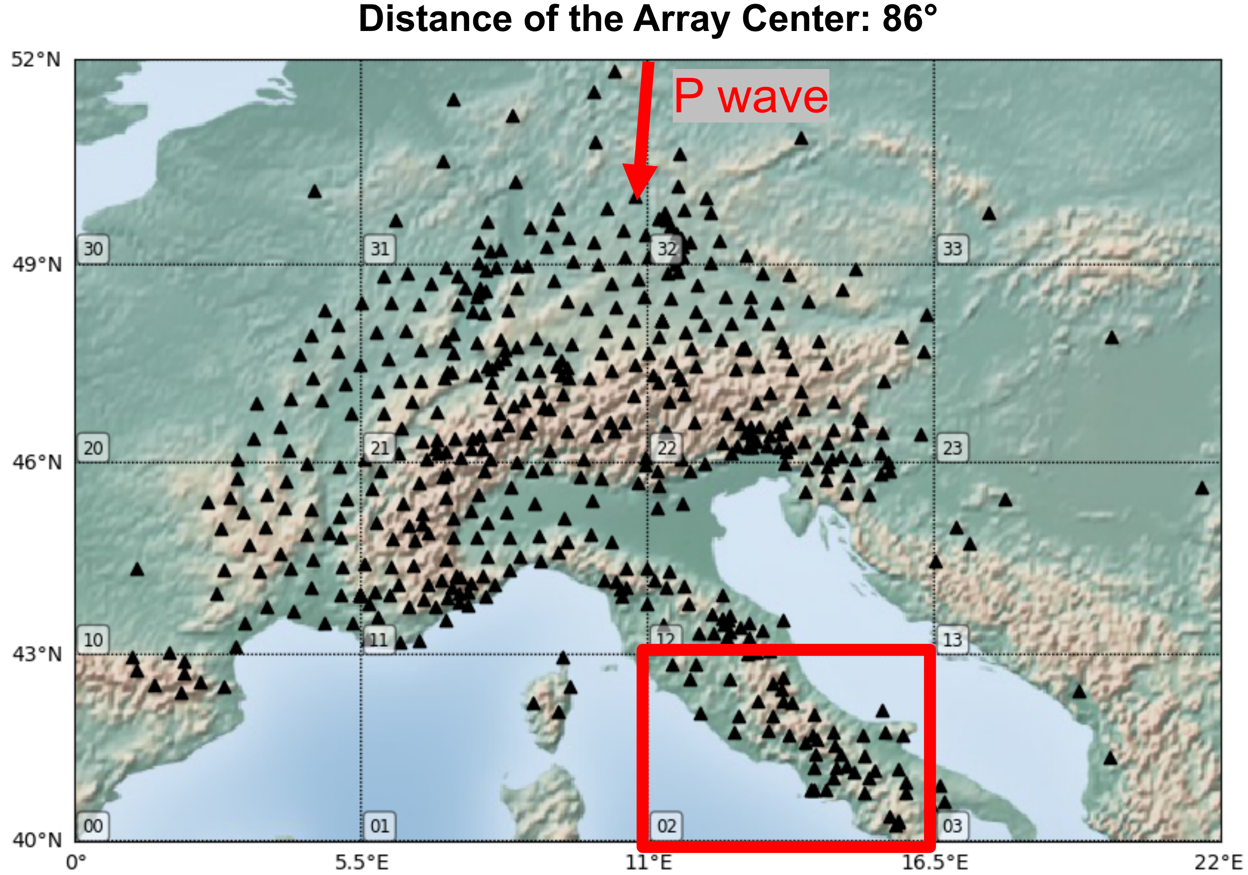

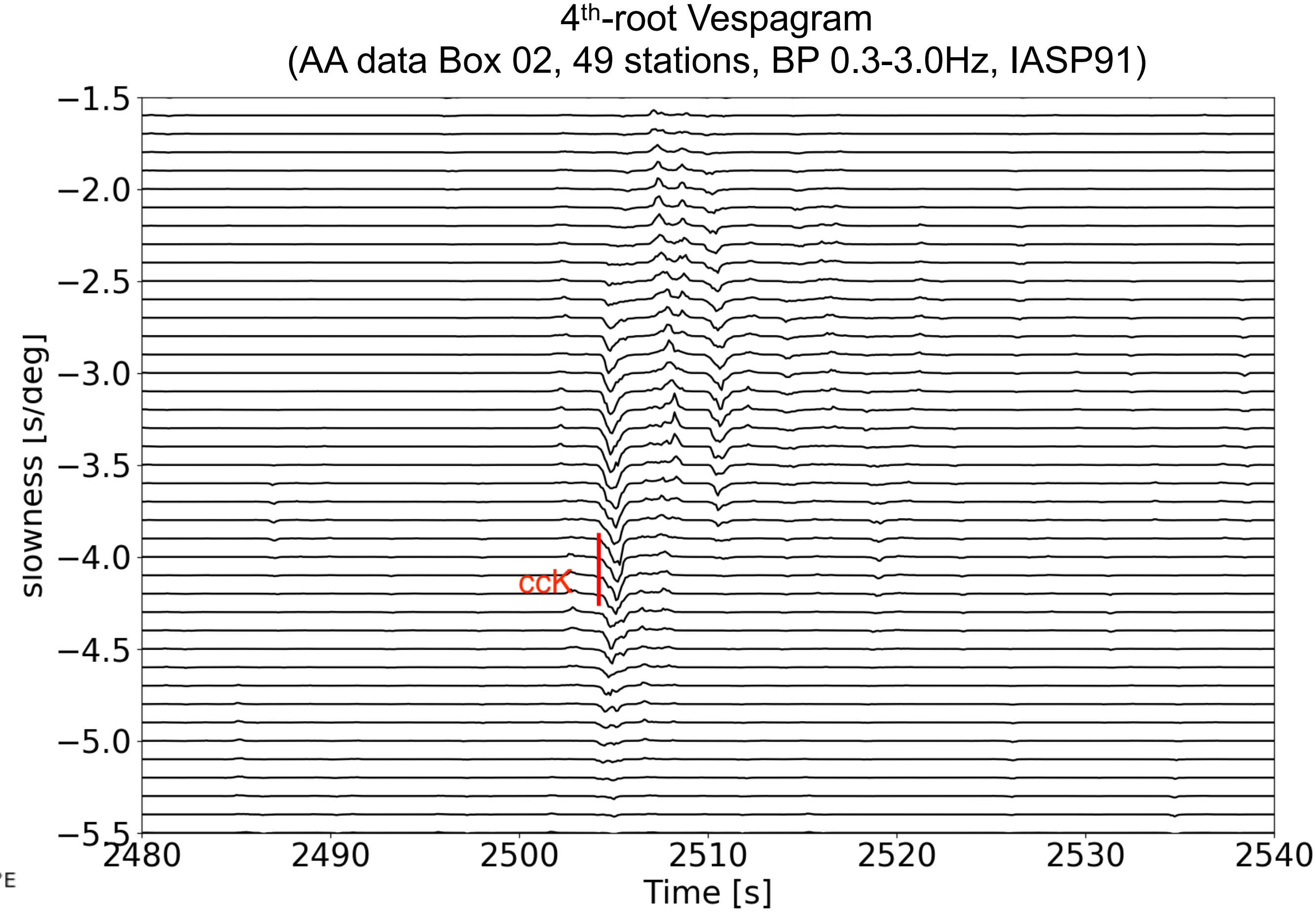

Figure 19: Here the subarray in a further distance is chosen. According to the theoretical travel time, SKP.K is not observed in distances beyond 85°. Only ccK is clearly observed. We can see all three phases in this event. Since the amplitude of SKP.K is much larger than ccK in general, it dominates the vespagram when it is computed with the whole array.

Observation vs. Non-observation of ccK/SKP.K

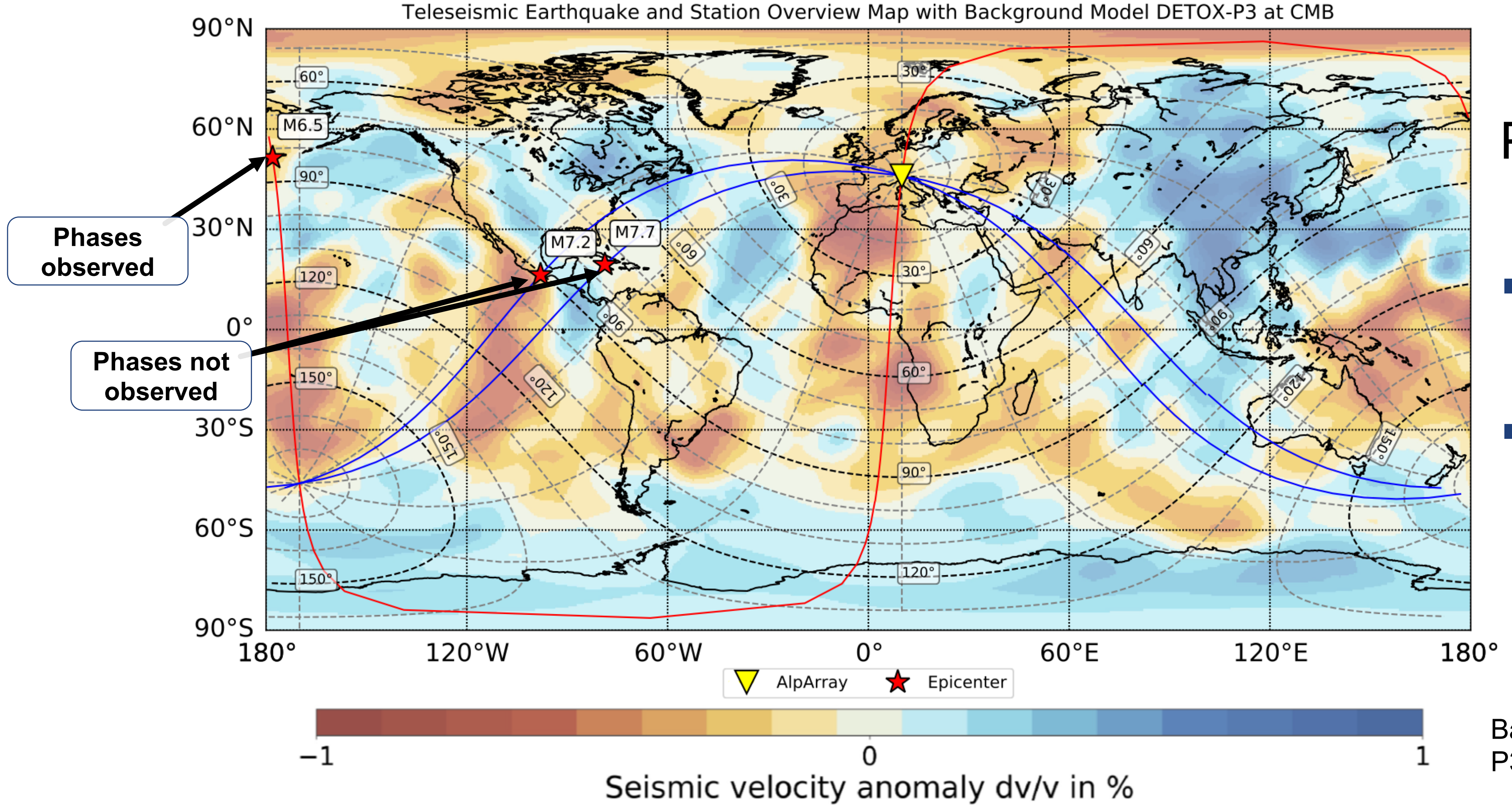

Possible explanations:

- CMB topography
- Lower mantle structures
  - LLSVP
  - ULVZ

Background tomographic model DETOX-P3 from *Hosseini et al., 2019* at the CMB.

Figure 20: However, these two phases are not observed in all examined events, for example, the events in Mexico and Cuba. To further investigate the observation and non-observation of these phases, one idea is to compare their interaction points at the CMB and see how the CMB topography and lower mantle structures influence these core phases.

Conclusion

We can identify core phases observed with AlpArray from both core-crossing and teleseismic distances by applying appropriate array processing techniques:

- **PKIKP and PKP**
  - Well-observed from core-crossing distances.
  - Observed waveforms show strong resemblance to the synthetics, which means that these core phases can be modelled accurately and included in seismic tomography.

- **Other high order core phases**
  - Present in teleseismic events.
  - Difficult to model because these phases have multiple reflections, but potentially help investigate the CMB topography and lower mantle structures.

Outlook

- Continue to download and process global events (≥ M5.8) between 2016 and 2019 recorded by AlpArray.
- Model P teleseismic and core phases with SCARDEC source-time functions.
- Result of the event and phase analysis will be presented in a statistical sense and contribute to the AlpArray community.

References

- AlpArray Seismic Network (2015): AlpArray Seismic Network (AASN) temporary component. AlpArray Working Group. Other/Seismic Network. doi:10.12686/alparray/z3_2015
- Hetényi, G., et al. (2018), The AlpArray Seismic Network: A Large-Scale European Experiment to Image the Alpine Orogen, Surveys in Geophysics, 39 (5), 1009-1033, DOI:10.1007/s10712-018-9472-4.
- Hosseini, K. (2016). Global multiple-frequency seismic tomography using teleseismic and core diffracted body waves. PhD Thesis, LMU München.
- Hosseini, K. and K. Sigloch (2015), Multifrequency measurements of core-diffracted P waves (Pdiff) for global waveform tomography. Geophysical Journal International, 203(1), 506-521, DOI:10.1093/gji/ggv298
- Hosseini, K. and K. Sigloch. (2017), ObspyDMT: a Python toolbox for retrieving and processing large seismological data sets, Solid Earth, 8, 1047-1070, DOI:10.5194/se-8-1047-2017
- Hosseini, K., et al. (2019), Global mantle structure from multifrequency tomography using P, PP and P-diffracted waves, Geophysical Journal International, 220 (1), 96-141, doi:10.1093/gji/ggz394.
- IRIS DMC (2015), Data Services Products: Synthetics Engine, doi:10.17611/DP/SYNGINE.1.
- Krischer, L., et al. (2015), ObsPy: a bridge for seismology into the scientific Python ecosystem, Computational Science & Discovery, 8 (1), 014,003, doi:10.1088/1749-4699/8/1/014003.
- Nissen-Meyer, T., et al. (2014), AxiSEM: broadband 3-D seismic wavefields in axisymmetric media. Solid Earth, 5, 425-445, DOI:10.5194/se-5-425-2014
- van Driel. M., et al. (2015), Instaseis: instant global seismograms based on a broadband waveform database. Solid Earth, 6, 01-717, DOI:10.5194/se-6-701-2015
- Zhao, D. (2019), Importance of later phases in seismic tomography, Physics of the Earth and Planetary Interiors, 296, 106,314.